Dihydroquinone Ansamycins: Toward Resolving the Conflict between Low in Vitro Affinity and High Cellular Potency of Geldanamycin Derivatives

Anna C. Maroney,* Juan J. Marugan, Tara M. Mezzasalma, Alexander N. Barnakov, Thomas A. Garrabrant, Larry E. Weaner, William J. Jones, Ludmila A. Barnakova, Holly K. Koblish, Matthew J. Todd, John A. Masucci, Ingrid C. Deckman, Robert A. Galemmo, Jr., and Dana L. Johnson

Johnson & Johnson Pharmaceutical Research & Development, L.L.C., Spring House, Pennsylvania 19477

Received December 7, 2005; Revised Manuscript Received February 13, 2006

ABSTRACT: Heat shock protein 90 (Hsp90) is critical for the maturation of numerous client proteins, many of which are involved in cellular transformation and oncogenesis. The ansamycins, geldanamycin (GA) and its derivative, 17-allylaminogeldanamycin (17-AAG), inhibit Hsp90. As such, the prototypical Hsp90 inhibitor, 17-AAG, has advanced into clinical oncology trials. GA and 17-AAG potently inhibit tumor cell proliferation and survival but have been reported to bind weakly to Hsp90 in vitro. Recent studies have suggested that the in vitro potency of ansamycins against Hsp90 may be enhanced in the presence of cochaperones. Here, we present evidence of an alternative explanation. Ansamycins reduced to their dihydroquinones in the presence of common reducing agents in vitro have approximately 40-fold greater affinity than the corresponding oxidized quinones. The dihydroquinone of 17-AAG is not generated in an aqueous environment in the absence of reducing agents but is produced in both tumor and normal quiescent epithelial cells. The reduced form of 17-AAG is differentiated from its oxidized form not only by the higher affinity for Hsp90 but also by a protracted K_{off} rate. Therefore, the in vivo accumulation of the high-affinity dihydroquinone ansamycins in tumor cells contributes to the antitumor activity of these compounds and alters our understanding of the active species driving the efficacy of this class of compounds.

Since the discovery of the antiproliferative activity of geldanamycin (GA),[1] a compound derived from broths of *Streptomyces hygroscopicus* (*1*), a number of analogues, specifically 17-allylaminogeldanamycin (17-AAG) being the most advanced, have entered into clinical trials with cancer patients (*2*−*5*). These compounds target the N-terminal ATP binding pocket of heat shock protein 90 (Hsp90) (*6*, *7*). Hsp90 is an abundant, ubiquitously expressed molecular chaperone involved in the maturation of multiple client proteins, many of which are involved in regulating cell signaling, proliferation, and survival (*8*, *9*). Hsp90 partners with multiple cochaperones during the maturation of client proteins and is dependent upon its ATPase activity to complete the cycle (*10*−*12*). Client proteins of Hsp90 include Her-2, polo-like kinase, Akt, EGFR, Src, Abl, c-Met, and Raf-1 which are currently being targeted for intervention within oncology drug discovery or in clinical development (*13*). Incongruent in vitro and cellular potencies of the ansamycins against Hsp90 activity have led many to question the apparent target and mechanism of these compounds as well as the active species in cells (*14*). The affinity of GA and its derivative 17-AAG for isolated full-length dimeric Hsp90 has been reported in the low micromolar range (*7*, *12*, *15*); however, the activities of these compounds toward inhibition of cell proliferation in a broad array of tumor cell lines are in the low nanomolar range (*14*, *16*, *17*).

Others have sought to resolve the in vitro to in vivo discrepancies in the activities of the ansamycins. Evidence that the affinity of the ansamycins for Hsp90 alters when in the presence of cochaperones has been offered as one possible explanation (*18*, *19*). Furthermore, the presence of Hsp90 complexed with its cochaperones has been shown to occur at a higher frequency in tumor cells as compared to normal epithelial or endothelial cells, and this may explain, in part, why ansamycins preferentially accumulate in tumors (*18*, *20*, *21*). An opposing explanation has been provided by studies which demonstrated that the intracellular concentration of 17-AAG in cultured tumor cells accumulates with exposure, allowing for far greater cellular concentrations relative to exogenous media (*14*). It was proposed from these studies that the actual concentration in cells is in the high micromolar range, consistent with previous reports of low in vitro affinity. Given the emerging importance of the target and this class of compounds in oncology, we sought to clarify the discrepancies between the in vitro and cellular activities. Herein, we offer an alternative explanation providing direct biochemical and cellular evidence that the reduction of the quinone moiety shared by these ansamycins to the dihydroquinone yields a compound with nanomolar affinity to Hsp90 in vitro and is further distinguished from the quinone parent compound by possessing an extended off-rate.

MATERIALS AND METHODS

Materials. GA and 17-AAG were purchased from InvivoGen Inc. (San Diego, CA). Radicicol was purchased from BIOMOL Research Laboratories Inc. (Plymouth Meeting,

* To whom correspondence should be addressed. Telephone: 215-628-5356. Fax: 215-628-5047. E-mail: amaroney@prdus.jnj.com.

[1] Abbreviations: GA, geldanamycin; 17-AAG, 17-allylaminogeldanamycin; dihydro-17-AAG, dihydroquinone 17-allylaminogeldanamycin; Hsp90, heat shock protein 90; DMSO, dimethyl sulfoxide; TCEP, tris-(2-carboxyethyl)phosphine; ANS, 1-anilino-8-naphthalenesulfonate.

10.1021/bi0524969 CCC: $33.50
Published on Web 04/07/2006

PA). [^{3}H]-17-AAG and [^{3}H]dihydro-17-AAG were obtained from Moravek Biochemicals (Brea, CA). DL-Dithiothreitol (DTT), tris(2-carboxyethyl)phosphine (TCEP), L-glutathione (GSH), ATP, ADP, AMPPNP, and ATPγS were purchased from Sigma-Aldrich (St. Louis, MO).

Reduction of 17-AAG to Dihydro-17-AAG. The dihydroquinone of 17-AAG (dihydro-17-AAG) was formed by dissolving 20 mg of 17-AAG in 4 mL of ethyl acetate followed by the addition of 7 mL of a 10% aqueous solution of sodium dithionite (*22*). The biphasic mixture was vigorously stirred under argon, and the reaction went to completion within 1.5 h, as determined by LC-MS. LS-MS/ELS was performed on a system consisting of an electrospray source on a Thermo-Finnigan LCQ mass spectrometer (San Jose, CA), a SEDEX 75C evaporative light scattering detector (Richard Scientific, Novato, CA), a Shimadzu LC-10ADvp binary gradient pumping system (Columbia, MD), a Gilson 215 (Middleton, WI) configured as an autosampler, and a SUPELCOSIL (3 μm, 3.3 cm $\times$ 2.1 mm) column (Sigma-Aldrich, St. Louis, MO). The flow rate was 0.5 mL/min with a linear gradient varied from 100% water with 0.05% trifluoroacetic acid to 100% acetonitrile with 0.05% trifluoroacetic acid in 6 min. After completion of the reaction, the mixture was poured into an extraction funnel and diluted with water (15 mL) and ethyl acetate (10 mL). The organic layer was washed three times with water and finally with brine. The organic layer was collected, dried (Na_2SO_4), filtered, and concentrated under vacuum. TCEP (10 molar excess relative to dihydro-17-AAG) was added to the residue, and the mixture was dissolved in DMSO to produce a 10 mM solution of dihydro-17-AAG containing 100 mM TCEP. This procedure was followed for producing both radiolabeled and unlabeled dihydro-17-AAG. Tubes containing dihydro-17-AAG were purged with nitrogen gas, aliquoted, and stored at -80 °C.

Cloning and Expression of N-Terminal Hsp90. DNA encoding amino acids 9−236 of human Hsp90α (rhHsp90α9−236) was optimized for *Escherichia coli* expression and synthesized by DNA2.0 (Menlo Park, CA). A *Bam*HI (GlySer) site was added prior to amino acid 9 and a *Not*I site was incorporated after the stop codon by PCR. The PCR fragment was subcloned into a modified pET28 vector containing a His tag followed by a TEV cleavage site and *Bam*HI(GlySer) and *Not*I sites for subcloning (Novagen, San Diego, CA). Expression was carried out in a BL21 RIL (DE3) strain by growth at 37 °C in Luria broth (GibcoBRL, Gaithersburg, MD) to an $OD_{600} = 0.6-0.8$, followed by addition of 0.1 mM IPTG and temperature reduction to 15 °C. Cells were harvested 15 h postinduction. Purification of His-tagged rhHsp90α9−236 was carried out using Ni-NTA affinity columns. The His tag was removed by digestion with His-tagged Tev protease, and the protein was repurified by passing through Ni-NTA columns.

ThermoFluor Affinity Binding Assay. Compounds were prepared as 10 mM stocks in 100% DMSO; nucleotides were prepared as 100 mM stock in 5 mM HEPES (pH 7.0). Ligands were serially diluted in their respective mother liquor at a 1:2 volume ratio, providing 11 concentrations per series, plus a 12th well containing only diluents. Compound dilutions (50 nL) were dispensed in duplicate to assay plates using a Cartesian Hummingbird (Genomics Solutions Inc., Ann Arbor, MI). ThermoFluor reactions contained 50 nL of compound in addition to 4 μL of 0.05 mg/mL (1.8 μM) rhHsp90α9−236 in 40 mM Hepes, pH 7.5, 100 mM KCl, 5 mM $MgCl_2$, and 1 mM EDTA, plus 60 μM 1-anilino-8-naphthalenesulfonate (ANS), and were overlayed with 1 μL of silicone oil to prevent evaporation. When included, stocks of reducing agents (DTT, TCEP, GSH) were made fresh and used at a final concentration of 1, 1, and 2.5 mM, respectively.

All ThermoFluor assays were performed as previously described (*23*) in 384 black well Abgene PCR plates (Rochester, NY). Plates were heated from 25 to 90 °C at ~1 °C/min, and images were collected at 1 °C intervals. To collect each data point, the plate was held at constant temperature for 20 s, then illuminated with 390 $\pm$ 20 nm light (Hamamatsu Photonics, Bridgewater, NJ), imaged for 20 s with the shutter closed, and then imaged for 20 s with the shutter open, using a CCD camera detecting emission at 475−525 nm. Fluorescence intensity at each temperature was determined by summing pixel intensity associated within each well and then subtracting the sum of the same pixels collected from the shutter-closed image.

Primary data (fluorescence intensity vs temperature) were fit to standard equations describing protein thermal stability as previously described (*23*). These equations give six fit parameters: fluorescence of the native protein at T_m, fluorescence of the non-native protein at T_m, the temperature dependence of these two fluorescences, the midpoint in the transition between native and non-native protein, and a parameter describing the shape of the curve. For reversibly unfolding reactions that are at equilibrium, this latter parameter is the van't Hoff enthalpy.

Binding affinity was calculated by examining the trend of T_m vs ligand concentration, as previously described (*23*). Such calculations are highly dependent on the parameter used for the protein unfolding enthalpy, $\Delta_U H_{T_m}$, and to a lesser extent the heat capacity of protein unfolding, $\Delta_U C_p$. For rhHsp90α9−236, the parameters used to simulate ligand dosing were 100 kcal/mol (from protein thermal stability experiments) and 3 kcal/(mol·K) based upon the protein sequence data (*24*), respectively. Binding affinities obtained by perturbations of protein stability are most accurate at the protein T_m and were extrapolated to physiologically relevant temperature (37 °C) using standard equations, assuming the binding enthalpy ($\Delta_b H_{37}$) and the temperature-independent heat capacity ($\Delta_b C_p$) were -5 kcal/mol and -200 cal/(mol·K), respectively.

Stability of 17-AAG and Dihydro-17-AAG in Aqueous Solution by HPLC. 17-AAG (10 mM in 100% DMSO) was diluted to 50 μM in H_2O and analyzed by HPLC after 0 or 8 h incubation at 25 °C in the absence or presence of 0.5 mM TCEP. The LC components employed were the Agilent 1100 Series operated at 20 μL/min through a Zorbax SB-C18 column (5 μm, 150 mm $\times$ 0.5 mm). The gradient varied from 97% of 0.1% formic acid in water to 100% of 0.1% formic acid in 90:10 acetonitrile:water in 6 min with a 2 min hold and then reequilibrated to starting conditions for 4 min. The UV absorbance was measured at 254 nm. Compound identities were verified by LC-MS/MS analyses on an Agilent XCT Plus ion trap mass spectrometer (Palo Alto, CA), and under reducing conditions the quinone and hyroquinone ansamycins form the major peaks.

Determination of Dissociation Constants by Equilibrium Dialysis Assays. All binding assays with rhHsp90α9−236 were carried out using either [^{3}H]-17-AAG or [^{3}H]dihydro-17-AAG (specific activity 20 Ci/mmol) as a ligand. Equilibrium dialysis was performed as described (*25*). For a typical assay, 100 μL of N-terminal Hsp90 in binding buffer was dialyzed against 15 mL of binding buffer (40 mM Hepes, pH 7.5, 100 mM KCl, 5 mM $MgCl_2$, 0.5 mM EDTA, with or without 1 mM TCEP) containing [^{3}H]-17-AAG varying in concentration from 0.1 to 8 nM for the dihydroquinone species and from 0.2 to 8 μM for the quinone 17-AAG. Assays with [^{3}H]dihydro-17-AAG were carried out in binding buffer containing 1 mM TCEP. The concentration of rhHsp90α9−236 was 50 nM and 4 μM, respectively. Dialysis was performed at 4 °C. Samples (10−20 μL) taken from dialysis bags and dialysis buffers were added to scintillation vials containing 1.0 mL of BCS scintillation cocktail (Amersham Biosciences, Piscataway, NJ). The vials were counted in a 1450 Microbeta Plus liquid scintillation counter (Perkin-Elmer, Wellesley, MA). At equilibrium (typically after ∼ 48 h), the amount of 17-AAG bound to rhHsp90α9−236 was determined from the differential of radioactivity inside the dialysis bags and in the dialysis buffers. Values for K_d were derived from Scatchard plots.

Determination of the Off-Rate of [^{3}H]-17-AAG and [^{3}H]-Dihydro-17-AAG from rhHsp90α9−236. (A) Competition Studies with 17-AAG. A solution containing 10 μM rhHsp90α9−236 and 20 μM [^{3}H]-17-AAG in binding buffer without TCEP were incubated for 30 min at room temperature. At initiation, a 100-fold excess of unlabeled 17-AAG was added to the solution, and 50 μL aliquots were applied at equal time intervals between 0.5 and 15 min on Bio-Rad MicroBio-Spin-6 chromatography columns previously equilibrated with binding buffer. Immediately after sample application the columns were centrifuged according to the protocol supplied by the manufacturer. Samples obtained during the time course were counted as described above. The data were normalized to the first time point (0.5 min), and a first-order exponential fit was calculated.

(B) Competition Studies with Dihydro-17-AAG. rhHsp90α9−236 (0.2 μM) and 0.4 μM [^{3}H]dihydro-17-AAG in binding buffer with 1 mM TCEP were incubated overnight at 4 °C. The solution was brought to room temperature for 1 h. At initiation, a 100-fold excess of unlabeled dihydro-17-AAG was added to the solution, and 50 μL aliquots were applied at equal time intervals between 5 min and 4.5 h on Bio-Rad MicroBio-Spin-6 chromatography columns previously equilibrated with binding buffer containing 1 mM TCEP. Centrifugation and counting steps were the same as described above for the 17-AAG. The data were normalized to the first point (0.5 h).

Viability Assays. MCF7 mammary carcinoma cells (HTB-22; ATCC, Manassas, VA) were grown in DMEM plus 10% FBS and seeded at 2000 cells per well in white-walled, clear bottom plates (3610; Corning Life Sciences, Acton, MA). After allowing for adherence overnight, cells were incubated with 17-AAG for 3 days and were subjected to CellTiter-Glo (Promega Corp., Madison, WI) for determination of viable cells under proliferating conditions. Human mammary epithelial cells (HMECs, CC-2551; Clonetics/Cambrex, East Rutherford, NJ) were grown in complete MEGM as recommended by the supplier. Cells were either seeded at 2−8000 cells per well (subconfluency) and treated 24 h later or seeded at 10000 cells per well (confluency) and grown for another 4 days to reach quiescence prior to treatment. The cells were dosed with 17-AAG for 3 days and were subjected to CellTiter-Glo for determination of viable cells. Data were analyzed using GraphPad Prism (version 4), and the 95% confidence limits for all data generated were within 2-fold.

Measurement of Dihydro-17-AAG in HMECs and MCF7 Cells. HMECs were plated at 50% confluency and refed growth media over a 10-day period until the plates reached confluency. MCF7 cells were grown to near confluency in 100 mm plates. Both cell lines were exposed to 10 μCi (0.37 MBq) of [^{3}H]-17-AAG at a concentration of 265 nM (3.3 μCi/mL) for 1 h at 37 °C. The cell monolayers were washed in cold PBS, extracted into 0.5 mL of isopropyl alcohol, and immediately frozen to −80 °C. Radiochromatograms of the extracts were obtained by HPLC analysis using an Agilent 1100 series system with a 4.6 (i.d.) by 250 mm Zorbax C8 column. The column was eluted using a linear gradient starting at 6% acetonitrile−formic acid (0.1%) in water−formic acid (0.1%) and increasing to 100% acetonitrile−formic acid over 6 min and then held at this composition for 10 min. The flow rate was 1 mL/min and column temperature 40 °C. Radioactive flow detection was completed with an IN/US Systems Inc. β-RAM detector equipped with a 0.5 mL liquid flow cell and EcoScint scintillation cocktail (National Diagnostics) flowing at 2 mL/min.

RESULTS

High-Affinity Binding of Ansamycins to Hsp90 in Vitro Is Dependent upon the Presence of Reducing Agents. ThermoFluor[2] binding technology was used to determine the association constants of compounds to rhHsp90α9−236. In this approach, an environmentally sensitive fluorescent dye (ANS) is used to monitor protein unfolding as a function of temperature; compound binding to target proteins is detected by measuring an increase in protein thermal stability (*23*). Addition of a fixed dose of GA to rhHsp90α9−236 increased the T_m from 50 to 57 °C (Figure 1A). A complete concentration response curve for GA revealed a K_d of 143 nM (Figure 1B), consistent with previously reported values (*26*−*28*). Multiple parameters were examined during the development of the affinity binding assay conditions including the addition of reducing agents. Whereas reducing agents had no effect on the thermal stability of rhHsp90α9−236 alone, addition of TCEP nearly doubled the amount of thermal energy needed to destabilize rhHsp90α9−236 in the presence of GA, increasing T_m even further (Figure 1). Likewise, the K_d of GA for rhHsp90α9−236 in the presence of TCEP was 48-fold higher in affinity, yielding a K_d of 3 nM (Figure 1B). Similar results were obtained in the presence of other reducing agents, such as DTT, and to a lesser extent with GSH (Table 1). Although full-length Hsp90 was unsuitable in the ThermoFluor assay since it did not possess a single cooperative unfolding transition, similar binding affinity in the presence of reducing agents was confirmed using a fluorescent-labeled GA probe (data not shown) (*28*). The

[2] The ThermoFluor assay was developed by 3-Dimensional Pharmaceuticals, Inc., which has been merged into Johnson & Johnson Pharmaceutical Research & Development, L.L.C. ThermoFluor is a trademark registered in the United States and certain other countries.

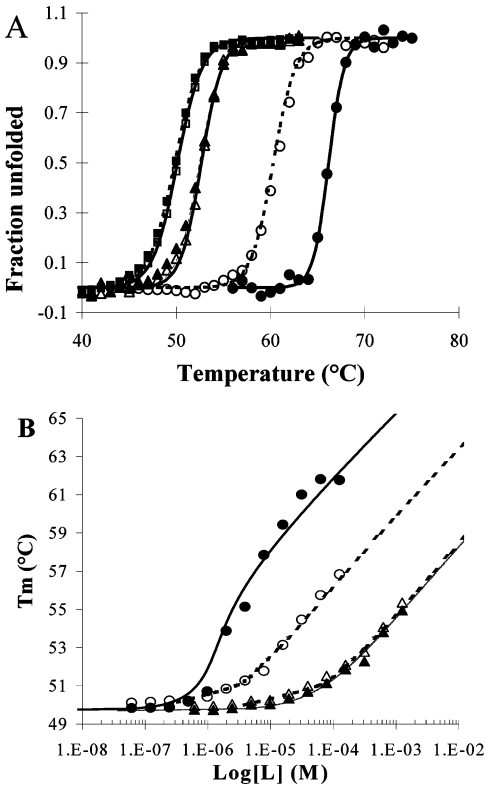

FIGURE 1: (A) Hsp90 protein stability as a function of temperature. The thermal stability of rhHsp90α9−236 (1.8 μM) was measured using ThermoFluor in buffer plus ANS dye (squares), with 312 μM ADP (triangles), or with 125 μM GA (circles) under standard conditions. Reactions included no TCEP (open symbols, dotted lines) or 1 mM TCEP (closed symbols, solid lines). Reactions were heated at 1 °C/min, and fluorescence intensity of the protein−ANS dye at 500 nm was measured using CCD. Data were normalized using standard equations, and the curve midpoint (T_m) was fit as previously described. (B) Dose-dependent changes in the T_m for GA and ADP binding to rhHsp90α9−236. Protein T_m was determined using the indicated concentrations of GA (circles) or ADP (triangles) in the absence (open symbols, dotted lines) or presence (closed symbols, solid lines) of 1 mM TCEP. Results shown represent averages from six separate experiments. Binding affinity was determined by fitting data to previously described equations (*23*).

Table 1: Affinity of Ansamycins and Nucleotides to rhHsp90α9−236 As Measured by ThermoFluor Microcalorimetry

	K_d (μM)			
compound	none	TCEP	DTT	GSH
17-AAG	2.0	0.05	0.10	1.25
dihydro-17-AAG	0.05	0.025	0.025	0.05
GA	0.143	0.003	0.005	0.025
dihydro-GA	0.005	0.001	0.005	0.003
radicicol	0.001	0.002	0.010	0.001
ATP	333	333	333	333
ATPγS	250	250	333	250
AMPPNP	500	500	500	500
ADP	50.0	50.0	55.6	50.0

relative K_d measured in the presence of a series of reducing reagents roughly paralleled the solution reduction potential (Table 1). Although structural analysis from cocrystallization of ansamycins with Hsp90 has proven that these compounds bind to the ATP pocket of Hsp90 (*6*, *29*), it cannot be determined if the structures correspond with the quinone or dihydroquinone form due to the resolution of the data. The higher in vitro affinity of GA in the presence of reducing agents was more consistent with the cellular potency reported for this compound (*30*).

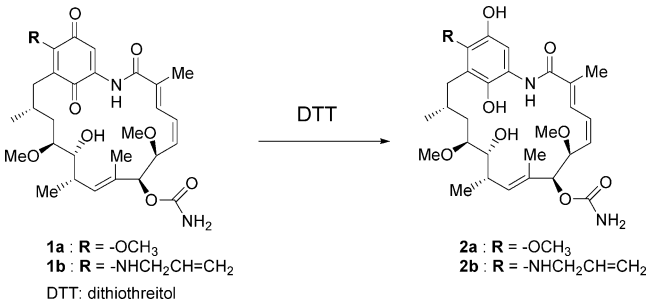

FIGURE 2: Reduction of ansamycins to their dihydroquinones by mild reducing agents such as DTT. GA (**1a**) or 17-AAG (**1b**) is reduced by DTT to their corresponding dihydro-GA (**2a**) or dihydro-17-AAG (**2b**) analogues.

The adenosine nucleotides have been reported to bind in the high micromolar range, wherein ADP has a greater affinity to Hsp90 than ATP (*10*, *27*, *31*). In this regard, the ΔT_m of rhHsp90α9−236 in the presence of a fixed concentration of ADP was 2.9 °C (Figure 1A) with a K_d of 50 μM (Figure 1B and Table 1). The K_d was not significantly affected by the presence of reducing agents, supporting that the phenomenon observed in the presence of GA was not a general occurrence.

As mentioned earlier, the large divergence in binding affinity of GA in the absence or presence of TCEP is of interest since it has long been recognized that the relatively low affinity of ansamycins for Hsp90 in vitro is inconsistent with their high cellular potency (*14*, *18*). Therefore, to test the general nature of the effect of reducing agents on equilibrium binding of ligands to rhHsp90α9−236, the affinity of additional active site directed molecules was tested with a panel of reducing agents (Table 1). Similar to GA, a 40-fold increase in affinity of 17-AAG, a structurally related analogue of GA, for rhHsp90α9−236 was observed in the presence of TCEP (Table 1). Radicicol, which is structurally unrelated to GA and does not contain the quinone moiety, bound to rhHsp90α9−236 with a K_d of 1 nM, consistent with previously reported values (*7*, *27*). However, the ThermoFluor concentration curves in the presence of all reducing agents were atypical with this compound. Further analysis of radicicol in the presence of DTT indicated that there was covalent modification of radicicol (data not shown). This is consistent with the report by others that radicicol forms a 1,6 adduct with DTT by Michael addition of the thiol of DTT to the α,β,γ,δ-unsaturated ketone of radicicol (*32*). Despite this complication, reducing agents did not change the overall affinity of radiciol for rhHsp90α9−236. Like nucleotide binding, reducing agents had no effect on radicicol affinity to rhHsp90α9−236, suggesting that the differences observed with the ansamycins were related to the reduction of the quinone moiety, which is unique to these molecules (Figure 2).

Equilibrium Binding of 17-AAG and Dihydro-17-AAG to rhHsp90α9−236. To confirm results observed in ThermoFluor, [^{3}H]-17-AAG and purified [^{3}H]dihydro-17-AAG (stored in 10-fold molar excess with TCEP) were added to rhHsp90α9−236 under conditions of equilibrium binding. Scatchard analysis of [^{3}H]-17-AAG binding to rhHsp90α9−236 produced a K_d of 1.1 μM whereas [^{3}H]dihydro-17-AAG

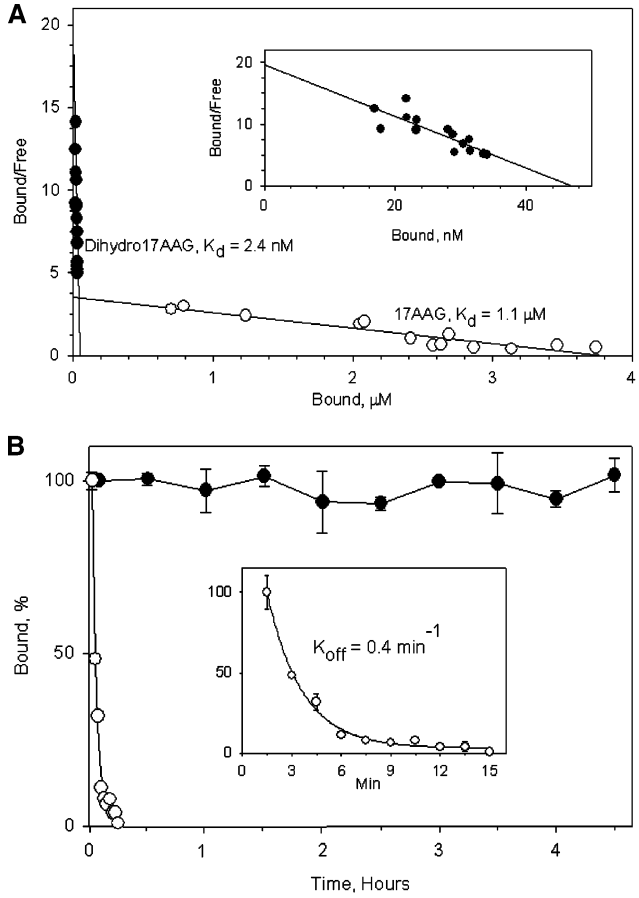

FIGURE 3: (A) Scatchard analysis of binding of [^{3}H]-17-AAG and [^{3}H]dihydro-17-AAG to rhHsp90α9−236. The data are representative from two equilibrium dialysis experiments for both 17-AAG and dihydro-17-AAG (open and closed circles, respectively). Linear regression fits provided K_d values of 1.1 μM for 17-AAG and 2 nM for dihydro-17-AAG. The inset shows the same data for dihydro-17-AAG with the horizontal axis in the nanomolar scale. (B) Dissociation of 17-AAG and dihydro-17-AAG from rhHsp90α9−236. [^{3}H]-17-AAG in binding buffer without TCEP (open circles) or [^{3}H]dihydro-17-AAG in binding buffer containing 1 mM TCEP (closed circle) were competed with either unlabeled 17-AAG or dihydro-17-AAG, respectively. Samples were extracted over the time course indicated, and radioactivity was captured by spin column chromatography. The inset shows the data for 17-AAG in the minute time scale with exponential fit.

bound with a K_d of 2.4 nM (Figure 3A). The micromolar affinity of 17-AAG is consistent with previously reported data using the filter binding assay (*27*). A shift to greater binding affinity of 17-AAG to rhHsp90α9−236 in the presence of TCEP confirmed the original ThermoFluor data (Table 1).

The ansamycins have been reported to accumulate preferentially in tumor tissue in vivo (*20*). Although several theories have been proposed, the mechanism of this accumulation remains controversial (*14*, *18*). One possible explanation, given our observation that dihydroquinone ansamycins have a greater affinity for Hsp90, is that these forms may also demonstrate differences in the association/dissociation rates for Hsp90 as compared to quinone ansamycins. Therefore, we examined the dissociation rate of 17-AAG and dihydro-17-AAG. The dissociation rate for 17-AAG was 0.4 min^{-1} (Figure 3B). The relatively fast K_{off} rate is consistent with a fast K_{on} rate previously reported for 17-AAG (*27*). In contrast, the dissociation rate for dihydro-17-AAG was so significantly prolonged such that a value could not be determined over the time period (4.5 h) of the experiment (Figure 3B). These data suggest that the dihydroquinone form of 17-AAG may be contributing to the accumulation observed in tumors.

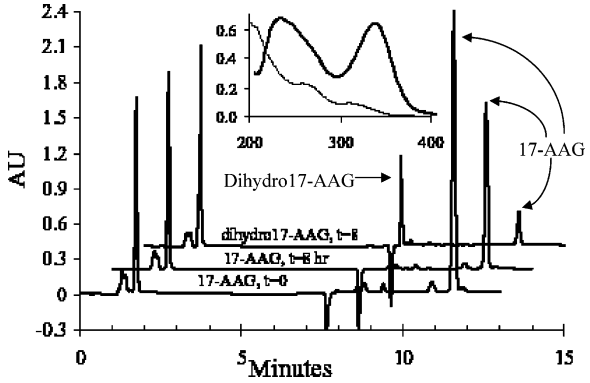

FIGURE 4: Stability of 17-AAG and dihydro-17-AAG by HPLC. 17-AAG (10 mM in 100% DMSO) was diluted to 50 μM in H_2O and analyzed by HPLC after 0 or 8 h incubation at 25 °C in the absence or presence of 0.5 mM TCEP. Under these conditions, 17-AAG elutes at ~11.5 min, whereas dihydro-17-AAG elutes at ~8 min. HPLC traces for each sample are shown offset by a 1 min interval for ease of viewing. Inset: UV/vis spectrum of 50 μM 17-AAG in buffer without (bold line) or with 1 mM DTT (thin line) showing the distinct spectral properties of 17-AAG and dihydro-17-AAG (*y*-axis, absorbance; *x*-axis, wavelength).

Stability of 17-AAG in an Aqueous Environment. It was of interest to determine whether the dihydroquinone form of the ansamycins occurs as a result of natural instability in an aqueous environment. Therefore, 17-AAG was suspended in serum-free medium containing 1% DMSO, and the quinone and dihydroquinone forms were separated by HPLC and tracked by UV absorption over time. The UV spectral analysis of the quinone and dihydroquinone forms of 17-AAG revealed absorption between 250 and 300 nm (Figure 4, inset), and detection of the two species was determined at 254 nm during the HPLC separation. The concentration of 17-AAG was approximately halved by 8 h; however, at no time was there evidence that dihydro-17-AAG was being formed (Figure 4). In the presence of 0.5 mM TCEP (10-fold molar excess relative to 17-AAG), approximately 70% of 17-AAG rapidly converts (within 0.5 h; data not shown) to the dihydroquinone, and in the presence of reducing agent this form is stable over 8 h (Figure 4). In conclusion, the high-affinity dihydro-17-AAG does not form spontaneously in aqueous solution without the assistance of a reducing agent.

Reduction of 17-AAG in Whole Cells. The lack of formation of dihydro-17-AAG in an aqueous environment suggested to us that if the high-affinity form of the compound were to play a physiological role in inhibiting Hsp90, then the formation of dihydro-17-AAG must occur within the cellular environment. Furthermore, ansamycins potently inhibit the growth of a wide variety of tumor cells in the low nanomolar range with little effect on the viability of quiescent normal endothelial and epithelial cells (*14*, *18*). One possible explanation for this effect is that the reduction of ansamycins in a tumor cell environment may be greater as compared to normal epithelial cells (*17*). To address these possibilities, we first examined the effect of 17-AAG on cell viability in MCF7 human breast cancer cells and primary

Table 2: Conversion of 17-AAG to Dihydro-17-AAG in HMECs and MCF7 Cells

	viability IC_{50} (μM)	% [^{3}H]-17-AAG	% [^{3}H]dihydro-17-AAG
media		94.7	5.2
MCF7 cells	0.128	31.5 ± 1.0	68.4 ± 1.0
proliferating HMECs	0.008	ND	ND
quiesced HMECs	>10	30.2 ± 0.8	69.7 ± 0.8

HMECs. The IC_{50} values for viability of MCF7 cells and proliferating HMECs were 128 and 8 nM, respectively, and greater than 10 μM in quiesced HMECs (Table 2). Similar differences between IC_{50} values of proliferating and quiesced cells were observed in normal human umbilical vein endothelial cells, clearly indicating that replicating cells were the more sensitive species (data not shown). We next determined whether the reduction of 17-AAG could be detected in these cells. An initial experiment examining the time course of conversion of 17-AAG to dihydro-17-AAG indicated that the reaction went to equilibrium within 1 h in MCF7 cells (data not shown). Therefore, media or MCF7 cells were incubated with 265 nM [^{3}H]-17-AAG for 1 h followed by lysis in ethanol. Due to concerns with stability, these samples were immediately applied to HPLC with an in-line radioactive detector. The extraction efficiency as detailed in the protocol was greater than 99%, and no change in specific activity occurred during the 1 h exposure of [^{3}H]-17-AAG in media alone (Table 2). Approximately 68% of [^{3}H]-17-AAG was found as the dihydroquinone in MCF7 cells, indicating that indeed reduction occurs in whole cells and therefore may be directly contributing to the cellular activity of ansamycins (Table 2). Reduction of 17-AAG took place in quiesced HMECs to the same extent as MCF7 cells; therefore, it is unlikely that the difference in cellular potency of ansamycins in tumors vs resting epithelial cells can be explained simply by a difference in reducing environment (Table 2). Overall, these results support that dihydro-17-AAG does form in cells and may play a physiological role in regulating tumor growth.

DISCUSSION

Geldanamycin and its derivatives represent a class of compounds that have profoundly influenced the oncology community in regard to the value of targeting the inhibition of Hsp90 for the treatment of cancer. These compounds are highly potent inhibitors of cell proliferation across a broad panel of tumor cells with average IC_{50}'s in the low nanomolar range (*17*, *33*−*35*). Such broad activity coupled to the evolving elemental understanding of how Hsp90 inhibitors block multiple oncogenic signaling pathways has guided the initial development of these compounds as cancer drugs. While the difficulties in formulating 17-AAG have to some extent been overcome with newer generations of more soluble compounds, all of the ansamycin derivatives being tested currently in the clinic are limited by intravenous administration and hepatic dose limiting toxicity related to the quinone moiety structurally shared by all of the derivatives (*4*, *5*, *36*−*39*). Therefore, a rationale to discover non-ansamycin Hsp90 inhibitors to avoid hepatotoxicity and potentially provide an oral route of administration for patients is highly attractive and well justified. Nevertheless, there is much to be learned from the preclinical history of these agents and the ongoing clinical studies with the ansamycins. Clearly, the progression of the concept that Hsp90 inhibitors will be clinically beneficial to cancer patients remains unfulfilled but highly compelling. In this light, we have sought to resolve the apparent conflict between in vitro and cellular potencies that have overshadowed the mechanism of action of the ansamycins.

Using a ThermoFluor affinity binding assay, our results confirm previous reports indicating that 17-AAG and GA have a submicromolar to low micromolar affinity to Hsp90 (Figure 1 and Table 1) (*26*−*28*). To our surprise, the dihydroquinone forms of ansamycins demonstrate substantially greater affinity to Hsp90 as compared to the quinone forms as determined by two different approaches (ThermoFluor microcalorimetry and filter binding sssays) (Figures 1 and 3A and Table 1). The effect of reducing agents appeared to be limited to the ansamycin class of compounds since the structurally unrelated inhibitor, radicicol, and ATP analogues do not contain the reducible quinone moiety and their affinities to Hsp90 are unaltered in the presence of reducing agents (Table 1).

Schnur and colleagues synthesized analogues of GA with modifications in the quinone ring and concluded on the basis of a structure−activity relationship that the quinone and not the dihydroquinone moiety was essential for cellular activity (*22*). They examined the degradation of the ErbB2 receptor in cells as an indication of active analogues. These authors compared cellular activities of GA derivatives with substitutions at the 18th position of the quinone ring. Modifications, such as acetylation, which cannot be reduced, were inactive in cells, whereas guanidine substitutions were active, leading to the conclusion that the dihydroquinone was not essential for activity. However, this study did not consider that intracellular reduction of the guanidine analogues might explain the cellular activity. We suggest that the reduction of the guanidine analogues was essential for cellular activity, consistent with the high affinity observed with dihydroquinone ansamycins reported herein (Table 1).

Recently, Kamal and colleagues provided in vitro evidence that the affinity of 17-AAG toward Hsp90 could be modulated by the addition of cochaperones, leading the authors to conclude that the multichaperone complex is essential for attaining a high-affinity state with 17-AAG (*18*). In the reported reconstitution studies of Kamal et al., no reducing agent was added with recombinant Hsp90 when examined alone. However, DTT was part of the purification protocol for the cochaperones as indicated by their references. Therefore, it is equally possible that the apparent increased affinity of Hsp90 for 17-AAG was due to the presence of reducing agent delivered with the cochaperones. Furthermore, no evidence was provided to demonstrate that complex formation was actually achieved in the reconstituted system (*18*). Additional evidence of an in vitro high-affinity site has also been demonstrated from binding studies measuring competition between GA linked to biotin and 17-AAG in the presence of tumor cell lysates followed by immunoprecipitation (*18*). Hereto, it is plausible that the tumor lysate provided a reducing environment to transform 17-AAG to dihydro-17-AAG similar to the effects reported here in MCF7 cells (Table 2).

Although reduction of the ansamycins may be a simple explanation resolving the difference between weak in vitro

affinity and strong cellular activity, it does not fully account for the differences in cellular potencies between tumor and resting normal cells (Table 2). Our initial findings indicate that the reduction of 17-AAG does not occur in an aqueous environment, suggesting that if the reduction were physiologically significant, it would need to convert within the context of the cellular environment (Figure 3). Indeed, reduction is observed in the MCF7 tumor cells; however, the quantitative formation of dihydro-17-AAG in MCF7 breast tumor cells is similar to the amount detected in normal quiesced HMECs (Table 2). The fact that reduction takes place in these cells at all supports the idea that the higher affinity dihydroquinone ansamycins are active metabolites that may contribute to cellular potency. However, since there is no quantitative discrimination in the rate of formation of dihydro-17-AAG in tumor or normal cell types, it cannot explain why others and we have observed lower potency toward viability in resting epithelial cells as compared to tumor cells (*14*, *18*). The dependency upon Hsp90 in the tumor environment may in part contribute to the distinct activities. We have confirmed the observation of Kamal et al. (*18*), demonstrating that the amount of Hsp90 complexed to cochaperones is higher in tumors than resting primary epithelial cells (data not shown). Therefore, a more likely scenario is that the quiesced cellular environment is less dependent upon complexed Hsp90 in contrast to replicating cells (Table 2).

Multiple studies in vivo have demonstrated that 17-AAG and its derivative 17-DMAG accumulate in tumor cells in comparison with other tissues (*20*, *37*). The accumulation appears to be peculiar to the ansamycins since it is not observed with other non-ansamycin Hsp90 inhibitors such as PU3 and PU24FCl (*14*). In an attempt to understand why this accumulation takes place, we hypothesized that there may be differences in the kinetics of binding of 17-AAG as compared to dihydro-17-AAG. Indeed, the K_{off} rate for dihydro-17-AAG is greatly protracted as compared to the rate of 17-AAG (Figure 3B). This, in part, may explain why 17-AAG can be found in tumor tissue at a time point when there are no detectable levels in the plasma (*37*).

It is well-known that solid tumors contain regions that grow under hypoxic conditions (*40*). In general, cells which survive in these hypoxic regions are resistant to radiotherapy and chemotherapy. A low oxygen environment favors formation of reduced products via reductases. Indeed, a prodrug strategy for developing hypoxia-selective cytotoxins is currently being tested in the clinic (*41*). In regard to GA and its derivatives, it has been previously shown that tumor cells expressing high levels of the reductase DT-diaphorase can increase tumor sensitivity to 17-AAG (*17*, *37*, *42*). DT-diaphorase levels in cells cultured in a dish appear to be sensitive to their microenvironment where higher expression is correlated with greater cell density (*43*, *44*). Our cell-based studies examining the conversion of 17-AAG to dihydro-17-AAG were performed under near to high density conditions in the two cell types examined. Although we cannot eliminate the possibility that there are varying levels of DT-diapharose in the cell lines reported herein, MCF7 cells are rich in DT-diaphorase activity (*45*), yet in our hands, 17-AAG is reduced to the same extent in this tumor cell line as compared to primary epithelial cells (Table 2). Indeed, the relevancy of DT-diapharose to sensitivity of 17-AAG in cancer patients is unclear. In a small clinical phase I sample population treated with 17-AAG no correlation between 17-AAG disposition or toxicity and the DT-diapharose (NQO1) genotype was observed (*5*). Overall, our results suggest a role for dihydroquinone ansamycins in the inhibition of Hsp90, and given the slow off-rate of this form of 17-AAG, it may also explain the selective in vivo accumulation of the ansamycins in tumors.

ACKNOWLEDGMENT

We acknowledge Keli Dzordorme for assistance in cloning rhHsp90α9−236.

REFERENCES

1. Uehara, Y. (2003) Natural product origins of Hsp90 inhibitors, *Curr. Cancer Drug Targets 3*, 325−330.
2. Sausville, E. A., Tomaszewski, J. E., and Ivy, P. (2003) Clinical development of 17-allylamino, 17-demethoxygeldanamycin, *Curr. Cancer Drug Targets 3*, 377−383.
3. Neckers, L., and Neckers, K. (2005) Heat-shock protein 90 inhibitors as novel cancer chemotherapeutics—an update, *Expert Opin. Emerging Drugs 10*, 137−149.
4. Grem, J. L., Morrison, G., Guo, X. D., Agnew, E., Takimoto, C. H., Thomas, R., Szabo, E., Grochow, L., Grollman, F., Hamilton, J. M., Neckers, L., and Wilson, R. H. (2005) Phase I and pharmacologic study of 17-(allylamino)-17-demethoxygeldanamycin in adult patients with solid tumors, *J. Clin. Oncol. 23*, 1885−1893.
5. Goetz, M. P., Toft, D., Reid, J., Ames, M., Stensgard, B., Safgren, S., Adjei, A. A., Sloan, J., Atherton, P., Vasile, V., Salazaar, S., Adjei, A., Croghan, G., and Erlichman, C. (2005) Phase I trial of 17-allylamino-17-demethoxygeldanamycin in patients with advanced cancer, *J. Clin. Oncol. 23*, 1078−1087.
6. Stebbins, C. E., Russo, A. A., Schneider, C., Rosen, N., Hartl, F. U., and Pavletich, N. P. (1997) Crystal structure of an Hsp90-geldanamycin complex: targeting of a protein chaperone by an antitumor agent, *Cell 89*, 239−250.
7. Roe, S. M., Prodromou, C., O'Brien, R., Ladbury, J. E., Piper, P. W., and Pearl, L. H. (1999) Structural basis for inhibition of the Hsp90 molecular chaperone by the antitumor antibiotics radicicol and geldanamycin, *J. Med. Chem. 42*, 260−266.
8. Csermely, P., Schnaider, T., Soti, C., Prohaszka, Z., and Nardai, G. (1998) The 90-kDa molecular chaperone family: structure, function, and clinical applications. A comprehensive review, *Pharmacol. Ther. 79*, 129−168.
9. Prodromou, C., and Pearl, L. H. (2003) Structure and functional relationships of Hsp90, *Curr. Cancer Drug Targets 3*, 301−323.
10. Obermann, W. M. J., Sondermann, H., Russo, A. A., Pavletich, N. P., and Hartl, F. U. (1998) In vivo function of Hsp90 is dependent on ATP binding and ATP hydrolysis, *J. Cell Biol. 143*, 901−910.
11. Grenert, J. P., Johnson, B. D., and Toft, D. O. (1999) The importance of ATP binding and hydrolysis by hsp90 in formation and function of protein heterocomplexes, *J. Biol. Chem. 274*, 17525−17533.
12. Panaretou, B., Prodromou, C., Roe, S. M., O'Brien, R., Ladbury, J. E., Piper, P. W., and Pearl, L. H. (1998) ATP binding and hydrolysis are essential to the function of the Hsp90 molecular chaperone in vivo, *EMBO J. 17*, 4829−4836.
13. Sreedhar, A. S., Soti, C., and Csermely, P. (2004) Inhibition of Hsp90: a new strategy for inhibiting protein kinases, *Biochim. Biophys. Acta 1697*, 233−242.
14. Chiosis, G., Huezo, H., Rosen, N., Mimnaugh, E., Whitesell, L., and Neckers, L. (2003) 17AAG: low target binding affinity and potent cell activity—finding an explanation, *Mol. Cancer Ther. 2*, 123−129.
15. Tian, Z. Q., Liu, Y., Zhang, D., Wang, Z., Dong, S. D., Carreras, C. W., Zhou, Y., Rastelli, G., Santi, D. V., and Myles, D. C. (2004) Synthesis and biological activities of novel 17-aminogeldanamycin derivatives, *Bioorg. Med. Chem. 12*, 5317−5329.
16. Whitesell, L., Shifrin, S. D., Schwab, G., and Neckers, L. M. (1992) Benzoquinonoid ansamycins possess selective tumoricidal activity unrelated to src kinase inhibition, *Cancer Res. 52*, 1721−1728.

17. Kelland, L. R., Sharp, S. Y., Rogers, P. M., Myers, T. G., and Workman, P. (1999) DT-Diaphorase expression and tumor cell sensitivity to 17-allylamino, 17-demethoxygeldanamycin, an inhibitor of heat shock protein 90, *J. Natl. Cancer Inst. 91*, 1940−1949.
18. Kamal, A., Thao, L., Sensintaffar, J., Zhang, L., Boehm, M. F., Fritz, L. C., and Burrows, F. J. (2003) A high-affinity conformation of Hsp90 confers tumour selectivity on Hsp90 inhibitors, *Nature 425*, 407−410.
19. Vilenchik, M. S. D., Basso, A., Huezo, H., Lucas, B., He, H., Rosen, N., Spampinato, C., Modrich, P., Chiosis, G. (2004) Targeting wide-range oncogenic transformation via PU24FCl, a specific inhibitor of tumor Hsp90, *Chem. Biol. 11*, 787−797.
20. Xu, L., Eiseman, J. L., Egorin, M. J., and D'Argenio, D. Z. (2003) Physiologically-based pharmacokinetics and molecular pharmacodynamics of 17-(allylamino)-17-demethoxygeldanamycin and its active metabolite in tumor-bearing mice, *J. Pharmacokinet. Pharmacodyn. 30*, 185−219.
21. Eiseman, J. L., Lan, J., Lagattuta, T. F., Hamburger, D. R., Joseph, E., Covey, J. M., and Egorin, M. J. (2005) Pharmacokinetics and pharmacodynamics of 17-demethoxy 17-[[(2-dimethylamino)ethyl]-amino]geldanamycin (17DMAG, NSC 707545) in C.B-17 SCID mice bearing MDA-MB-231 human breast cancer xenografts, *Cancer Chemother. Pharmacol. 55*, 21−32.
22. Schnur, R. C., Corman, M. L., Gallaschun, R. J., Cooper, B. A., Dee, M. F., Doty, J. L., Muzzi, M. L., Moyer, J. D., DiOrio, C. I., Barbacci, E. G., et al. (1995) Inhibition of the oncogene product p185erbB-2 in vitro and in vivo by geldanamycin and dihydrogeldanamycin derivatives, *J. Med. Chem. 38*, 3806−3812.
23. Matulis, D., Kranz, J. K., Salemme, F. R., and Todd, M. J. (2005) Thermodynamic stability of carbonic anhydrase: measurements of binding affinity and stoichiometry using ThermoFluor, *Biochemistry 44*, 5258−5266.
24. Robertson, A. D., and Murphy, K. P. (1997) Protein structure and the energetics of protein stability, *Chem. Rev. 97*, 1251−1268.
25. Barnakov, A. N., Barnakova, L. A., and Hazelbauer, G. L. (2002) Allosteric enhancement of adaptational demethylation by a carboxyl-terminal sequence on chemoreceptors, *J. Biol. Chem. 277*, 42151−42156.
26. Patel, K., Piagentini, M., Rascher, A., Tian, Z.-Q., Buchanan, G. O., Regentin, R., Hu, Z., Hutchinson, C. R., and McDaniel, R. (2004) Engineered biosynthesis of geldanamycin analogs for Hsp90 inhibition, *Chem. Biol. 11*, 1625−1633.
27. Carreras, C. W., Schirmer, A., Zhong, Z., and Santi, D. V. (2003) Filter binding assay for the geldanamycin-heat shock protein 90 interaction, *Anal. Biochem 317*, 40−46.
28. Kim, J., Felts, S., Llauger, L., He, H., Huezo, H., Rosen, N., and Chiosis, G. (2004) Development of a fluorescence polarization assay for the molecular chaperone Hsp90, *J. Biomol. Screening 9*, 375−381.
29. Jez, J. M., Chen, J. C., Rastelli, G., Stroud, R. M., and Santi, D. V. (2003) Crystal structure and molecular modeling of 17-DMAG in complex with human Hsp90, *Chem. Biol. 10*, 361−368.
30. Neckers, L., Schulte, T. W., and Mimnaugh, E. (1999) Geldanamycin as a potential anti-cancer agent: Its molecular target and biochemical activity, *Invest. New Drugs 17*, 361−373.
31. McLaughlin, S. H., Ventouras, L. A., Lobbezoo, B., and Jackson, S. E. (2004) Independent ATPase activity of Hsp90 subunits creates a flexible assembly platform, *J. Mol. Biol. 344*, 813−826.
32. Agatsuma, T., Ogawa, H., Akasaka, K., Asai, A., Yamashita, Y., Mizukami, T., Akinaga, S., and Saitoh, Y. (2002) Halohydrin and oxime derivatives of radicicol: synthesis and antitumor activities, *Bioorg. Med. Chem. 10*, 3445−3454.
33. Gorre, M. E., Ellwood-Yen, K., Chiosis, G., Rosen, N., and Sawyers, C. L. (2002) BCR-ABL point mutants isolated from patients with imatinib mesylate-resistant chronic myeloid leukemia remain sensitive to inhibitors of the BCR-ABL chaperone heat shock protein 90, *Blood 100*, 3041−3044.
34. Nimmanapalli, R., O'Bryan, E., Huang, M., Bali, P., Burnette, P. K., Loughran, T., Tepperberg, J., Jove, R., and Bhalla, K. (2002) Molecular characterization and sensitivity of STI-571 (imatinib mesylate, Gleevec)-resistant, Bcr-Abl-positive, human acute leukemia cells to SRC kinase inhibitor PD180970 and 17-allylamino-17-demethoxygeldanamycin, *Cancer Res. 62*, 5761−5769.
35. Xie, Q., Gao, C. F., Shinomiya, N., Sausville, E., Hay, R., Gustafson, M., Shen, Y., Wenkert, D., and Woude, G. F. (2005) Geldanamycins exquisitely inhibit HGF/SF-mediated tumor cell invasion, *Oncogene 24*, 3697−3707.
36. Hollingshead, M., Alley, M., Burger, A. M., Borgel, S., Pacula-Cox, C., Fiebig, H.-H., and Sausville, E. A. (2005) In vivo antitumor efficacy of 17-DMAG (17-dimethylaminoethylamino-17-demethoxygeldanamycin hydrochloride), a water-soluble geldanamycin derivative, *Cancer Chemother. Pharmacol. 56*, 115−125.
37. Banerji, U., Walton, M., Raynaud, F., Grimshaw, R., Kelland, L., Valenti, M., Judson, I., and Workman, P. (2005) Pharmacokinetic-pharmacodynamic relationships for the heat shock protein 90 molecular chaperone inhibitor 17-allylamino, 17-demethoxygeldanamycin in human ovarian cancer xenograft models, *Clin. Cancer Res. 11*, 7023−7032.
38. Behrsing, H. P., Amin, K., Ip, C., Jimenez, L., and Tyson, C. A. (2005) In vitro detection of differential and cell-specific hepatobiliary toxicity induced by geldanamycin and 17-allylaminogeldanamycin in rats, *Toxicol. in Vitro 19*, 1079−1088.
39. Smith, V., Sausville, E. A., Camalier, R. F., Fiebig, H.-H., and Burger, A. M. (2005) Comparison of 17-dimethylaminoethylamino-17-demethoxy-geldanamycin (17DMAG) and 17-allylamino-17-demethoxygeldanamycin (17AAG) in vitro: effects on Hsp90 and client proteins in melanoma models, *Cancer Chemother. Pharmacol. 56*, 126−137.
40. Brown, J. M., and Wilson, W. R. (2004) Exploiting tumour hypoxia in cancer treatment, *Nat. Rev. Cancer 4*, 437−447.
41. Patterson, L. H., McKeown, S. R., Robson, T., Gallagher, R., Raleigh, S. M., and Orr, S. (1999) Antitumour prodrug development using cytochrome P450 (CYP) mediated activation, *Anticancer Drug Des. 14*, 473−486.
42. Guo, W., Reigan, P., Siegel, D., Zirrolli, J., Gustafson, D., and Ross, D. (2005) Formation of 17-allylamino-demethoxygeldanamycin (17-AAG) hydroquinone by NAD(P)H:quinone oxidoreductase 1: role of 17-AAG hydroquinone in heat shock protein 90 inhibition, *Cancer Res. 65*, 10006−10015.
43. Bello, R. I., Gomez-Diaz, C., Navarro, F., Alcain, F. J., and Villalba, J. M. (2001) Expression of NAD(P)H:quinone oxidoreductase 1 in HeLa cells: role of hydrogen peroxide and growth phase, *J. Biol. Chem. 276*, 44379−44384.
44. Phillips, R. M., de la Cruz, A., Traver, R. D., and Gibson, N. W. (1994) Increased activity and expression of NAD(P)H:quinone acceptor oxidoreductase in confluent cell cultures and within multicellular spheroids, *Cancer Res. 54*, 3766−3771.
45. Fisher, G. R., and Gutierrez, P. L. (1991) The reductive metabolism of diaziquone (AZQ) in the S9 fraction of MCF-7 cells: free radical formation and NAD(P)H:quinone-acceptor oxidoreductase (DT-diaphorase) activity, *Free Radical Biol. Med. 10*, 359−370.

BI0524969